Asian Journal of Chemistry; Vol. 38, No. 9 (2026), 2447-2454
ASIAN JOURNAL OF CHEMISTRY
https://doi.org/10.14233/ajchem.2026.35949

Green Synthesis and Biological Evaluation of Silver Nanoparticles from *Leucas aspera* Leaf Extract with Phytochemical Profiling, Antibacterial and Anticancer Potential against Laryngeal Cancer

S. MEGALA[1,*], S.R. PARANTHAMAN[2], A. RAJABHUVANESWARI[3], SARAVANAN ALAMELU[4], G. RAM KUMAR[1], M.K. SRINIVASAN[5], KARUMUDI SINDHU[6], K. SHAGIRTHA[7,*] and K. AKSHAYA[8]

[1]PG and Research Department of Microbiology, St. Joseph's College of Arts and Science (Autonomous), Cuddalore-607001, India
[2]PG Department of Microbiology & Biotechnology, PERI College of Arts and Science, PERI IT Park, Manivakkam Tambaram-600048, India
[3]Department of Chemistry, Karpaga Vinayaga College of Engineering & Technology, Padalam-603308, India
[4]Department of Biochemistry and Biotechnology, Faculty of Science, Annamalai University, Chidambaram-608002, India
[5]Department of ENT, Saveetha Medical College and Hospitals, Saveetha Institute of Medical and Technical Sciences (SIMATS), Saveetha University, Chennai-602105, India
[6]Department of General Medicine, Saveetha Medical College and Hospitals, Saveetha Institute of Medical and Technical Sciences (SIMATS), Saveetha University, Chennai-602105, India
[7]PG and Research Department of Biochemistry, St. Joseph's College of Arts and Science (Autonomous), Cuddalore-607001, India
[8]Department of Bio-medical Engineering, Surya Engineering College, Erode-638107, India

*Corresponding authors: E-mail: megalasivaprakasam@gmail.com; shagirtha@gmail.com

Received: 11 March 2026 *Accepted*: 17 August 2026 *Published online*: 5 September 2026 AJC-22473

The present study aimed to synthesize and characterize biogenic silver nanoparticles (AgNPs) using an aqueous leaf extract of *Leucas aspera* and evaluate their antibacterial and anticancer activities. Phytochemical screening revealed flavonoids, phenols, alkaloids, tannins, saponins, carbohydrates, glycolysis-related compounds and steroids. GC-MS analysis identified 25 phytoconstituents, including lupeol, β-sitosterol, γ-linolenic acid, palmitic acid, stearic acid and retinyl palmitate, which may contribute to AgNPs formation and biological activity. UV-Visible spectroscopy confirmed AgNPs formation through a characteristic SPR band at 415 nm, while XRD revealed a face-centered cubic crystalline structure with an average crystallite size of 86.08 nm. FTIR analysis indicated the involvement of phenolic and flavonoid functional groups in Ag^+ reduction and nanoparticle stabilization. SEM, EDX, DLS and zeta potential analyses revealed near-spherical nanoparticles with an average particle size of 65.82 nm, hydrodynamic diameter of 118.74 nm, negative surface charge of -26.78 mV and 64.27 wt.% Ag composition. The synthesized AgNPs exhibited concentration-dependent antibacterial activity against *Staphylococcus aureus* and *Pseudomonas aeruginosa*, with MIC and MBC values of 100 and 125 µg/mL, respectively. Furthermore, AgNPs showed enhanced cytotoxicity against HEp-2 laryngeal carcinoma cells with an IC_{50} value of 236.63 µg/mL.

Keywords: *Leucas aspera*, Silver nanoparticles, Laryngeal cancer cells, Antibacterial activity, Anticancer activity, GC-MS.

INTRODUCTION

Recent advances in nanotechnology have influenced a wide range of scientific and biomedical research areas, with metallic nanoparticles receiving particular attention due to their distinctive physico-chemical properties and broad functional potential. Among these nanomaterials, silver nanoparticles (AgNPs) have emerged as important candidates for biomedical applications, particularly in antimicrobial therapy, wound management, medical textiles, diagnostic systems and cancer research [1]. Their nanoscale dimensions, large specific surface area, surface reactivity and ability to interact with biological molecules contribute to their diverse biological activities. AgNPs have been investigated for their potential use in cancer diagnosis and therapy, where their optical, chemical and biological properties provide opportunities for developing nanomedicine-based approaches [1,2].

Conventional physical and chemical routes for the synthesis of AgNPs often require high energy input, elevated temperatures or pressures and chemical reducing or stabilizing agents that may be toxic, costly or environmentally persistent. Such requirements have encouraged the development of greener

synthesis strategies, which minimize hazardous reagents and simplify nanoparticle production. Plant-mediated synthesis has gained considerable interest as a relatively simple, economical and environmentally compatible approach. Plant extracts contain a variety of naturally occurring phytochemicals, such as phenolics, flavonoids, terpenoids, alkaloids, proteins, sugars and other reducing constituents, which can participate in the reduction of Ag^+ ions and subsequent stabilization of the resulting nanoparticles [3]. The use of aqueous plant extracts can further reduce the dependence on hazardous organic solvents and provide a practical route for the preparation of boilogically functionalized AgNPs.

AgNPs possess physico-chemical characteristics that support their application across the food, pharmaceutical, healthcare and consumer-product sectors. Their antimicrobial properties have led to their incorporation into biomedical devices, wound dressings, coatings and textile materials [4,5]. Their interaction with cellular components and ability to generate biologically active species have attracted considerable interest in cancer-related research, where AgNPs are being explored as potential agents for selective cytotoxicity, cellular imaging, drug delivery and therapeutic intervention [2]. The biological performance of plant-mediated AgNPs can be influenced by particle size, morphology, surface chemistry, aggregation state and the phytochemical residues associated with their surfaces.

Leucas aspera (Lamiaceae), commonly known as thumbai, is a widely distributed herb found across several regions of the Indian subcontinent. It is an erect, robust herb with a characteristically quadrangular stem and generally reaches a height of approximately 15-60 cm. The leaves are sessile to shortly petiolate, linear-lanceolate, glabrous and possess an entire to crenate margin. The plant bears white, sessile flowers arranged toward the terminal regions of the branches. *L. aspera* has a long history of traditional use and has been employed for medicinal and insecticidal purposes [6]. Phytochemical investigations have identified several bioactive constituents in different parts of the plant such as β-sitosterol, ursolic acid, oleanolic acid, diterpenes, isopimarane glycosides, nectandrin B, maslinic acid, asperphenamate, isololiolide and linifolioside. The presence of such metabolites provides a chemical basis for investigating *L. aspera* as a biological source of reducing and capping constituents in nanoparticle synthesis.

The phytochemical richness of *L. aspera* leaves makes them suitable for green AgNPs synthesis. Its aqueous extract provides phytoconstituents that facilitate Ag^+ reduction and nanoparticle stabilization, offering a simple, cost-effective and eco-friendly synthesis route with reduced chemical use [3]. The present study was undertaken to investigate the phytochemical profile of *L. aspera* leaves and to synthesize AgNPs using their aqueous extract through a green synthesis route. The synthesized AgNPs were characterized by various analytical techniques to establish their physico-chemical properties, structural features, surface characteristics and optical behaviour. Their antibacterial activity was evaluated against selected pathogenic bacterial strains to assess their potential as antimicrobial nanomaterials. The cytotoxic potential of the synthesized AgNPs was further investigated against the HEp-2 laryngeal carcinoma cell line to assess their relevance to cancer related biomedical applications.

EXPERIMENTAL

Collection of plant material: Fresh and healthy leaves of *L. aspera* were collected from areas around Cuddalore (11.7442º N, 79.7675º E), India. The plant material was authenticated by a botanist at Annamalai University. The leaves were thoroughly washed with tap water followed by distilled water to remove dust, debris and microbial contaminants. They were shade-dried at ambient temperature (25 ± 2 ºC) for 10-14 days to minimize degradation of thermolabile phytochemicals. The dried leaves were finely powdered using a sterile electric grinder, passed through a 40-mesh sieve and stored in airtight glass containers under dry and dark conditions until further use.

Aqueous extraction of *L. aspera* leaves: For aqueous extraction, 20 g of dried leaf powder was mixed with 200 mL of distilled water and heated at 70 ºC for 30 min under continuous stirring. After cooling, the mixture was filtered through muslin cloth and Whatman No. 1 filter paper, followed by centrifugation at 5,000 rpm for 10 min. The clear supernatant was concentrated under reduced pressure at 40 ºC using a rotary vacuum evaporator and stored at 4 ºC in sterile amber bottles until phytochemical analysis, GC-MS profiling and AgNP synthesis.

Phytochemical screening: Qualitative phytochemical screening was performed using standard biochemical methods described by Harborne [7] and Evans [8]. Alkaloids were detected using Mayer's and Dragendorff's reagents, while flavonoids were identified by alkaline reagent and lead acetate tests. Tannins were assessed using $FeCl_3$ and lead acetate tests and saponins were detected by the frothing test. Phenols and terpenoids were examined using the $FeCl_3$ and Salkowski's tests, respectively, while glycosides were identified by the Keller-Killiani test. The intensity of colour development or precipitate formation was recorded as a qualitative indication of the presence and relative abundance of the respective phytochemical groups.

GC-MS analysis: Gas chromatography-mass spectrometry (GC-MS) analysis was performed to identify the phytochemical constituents present in the aqueous leaf extract of *L. aspera*. The extract was filtered through a 0.22 μm membrane filter prior to GC-MS analysis. No chemical derivatization was performed before analysis. The analysis was carried out using a GC-MS system equipped with a capillary column (30 m × 0.25 mm internal diameter, 0.25 μm film thickness) using helium as the carrier gas at a constant flow rate of 1.0 mL/min. The injection volume was 1 μL with a split ratio of 10:1 and the injector temperature was maintained at 250 ºC. The oven temperature was programmed initially at 50 ºC for 2 min, increased to 150 ºC at a rate of 10 ºC/min and held for 5 min, followed by a further increase to 280 ºC at 10 ºC/min with a final hold time of 10 min. The mass spectrometer was operated in electron ionization mode at 70 eV with a mass scan range of 50-600 *m/z*. The total chromatographic run time was approximately 45 min. The detected compounds were identified by comparing their mass spectra with reference spectra available in the NIST mass spectral library. Compound identification was based on spectral similarity matching, retention time comparison and molecular ion fragmentation patterns.

Only compounds showing acceptable library matching scores were considered for phytochemical identification.

Green synthesis of AgNPs: Green synthesis of AgNPs was carried out by mixing 10 mL of the aqueous leaf extract with 90 mL of 1 mM $AgNO_3$ solution under sterile conditions. The mixture was incubated at 37 ºC for 24 h in the dark to prevent photoreduction of Ag ions. A visual colour changes from pale yellow to dark brown confirmed the reduction of Ag^+ to Ag^0 nanoparticles. The solution was then centrifuged at 12,000 rpm for 20 min and the AgNP pellet was washed thrice with distilled water to remove unbound phytochemicals, followed by drying at 60 ºC for further characterization [9].

Characterization: The synthesized AgNPs were characterized using complementary analytical techniques. UV-Visible spectroscopy was performed using a JASCO V-650 UV-Visible spectrophotometer over 200-800 nm to identify the characteristic surface plasmon resonance (SPR) band. FTIR spectroscopy was carried out using a NICOLET 6700 FTIR spectrometer (Thermo-Fisher Scientific) over 4000-400 cm^{-1} to identify functional groups associated with Ag^+ reduction and nanoparticle stabilization. XRD analysis was performed using a Bruker D8 Advance X-ray diffractometer with Cu*K*α radiation (λ = 1.5406 Å) over a 2θ range of 20-80º to determine the crystalline structure and estimate the average crystallite size using the Debye-Scherrer equation. FE-SEM coupled with EDX was conducted using a Carl Zeiss Ultra Plus field-emission scanning electron microscope to examine the morphology and particle size, while EDX was used to determine the elemental composition and confirm the presence of silver. DLS analysis was performed using a Malvern Zetasizer Nano ZS90 to determine the hydrodynamic particle size and polydispersity index of the AgNPs suspension. Zeta potential measurements were obtained using the same Malvern Zetasizer Nano ZS90 to assess surface charge and colloidal stability.

Antimicrobial activity: The antimicrobial activity of the synthesized AgNPs was evaluated against *S. aureus* (Gram positive) and *P. aeruginosa* (Gram negative) using the agar diffusion method. Inoculated Mueller-Hinton agar plates were prepared and wells were loaded with 50 µL of AgNPs. The zones of inhibition were measured after incubation at 37 ºC for 24 h and compared to those of standard antibiotics [10].

Minimum inhibitory concentration and minimum bactericidal concentration assay: The antibacterial activity of green synthesized AgNPs using aqueous leaf extract of *L. aspera* was evaluated against *S. aureus* and *P. aeruginosa* by determining the minimum inhibitory concentration (MIC) and minimum bactericidal concentration (MBC). The MIC assay was performed using the broth microdilution method. Briefly, overnight bacterial cultures were prepared in Mueller-Hinton broth and adjusted to approximately 0.5 McFarland standard (~1.5×10^8 CFU/mL), followed by dilution to obtain a final inoculum concentration of ~5×10^5 CFU/mL. Different concentrations of *L. aspera*-mediated AgNPs (10, 15, 20 and 25 µL) were added to bacterial suspensions in sterile 96-well microtiter plates and incubated at 37 ºC for 18-24 h. The lowest concentration showing complete inhibition of visible bacterial growth was recorded as the MIC. For MBC determination, aliquots from MIC assay wells showing no visible growth were streaked onto Mueller-Hinton agar plates and incubated at 37 ºC for 18-24 h. The lowest concentration that resulted in complete absence of bacterial colonies was considered the MBC. The bactericidal efficiency of AgNPs was determined by calculating the MBC/MIC ratio, where a ratio ≤ 2 indicated bactericidal activity.

Anticancer activity (MTT assay): The cytotoxicity of AgNPs was assessed on human laryngeal cancer cells (HEp-2) using the MTT assay. Cells were incubated with varying concentrations of *L. aspera* leaf aqueous extract and AgNPs for 24 h and cell viability was measured by the reduction of MTT to formazan. IC_{50} values were determined based on dose-response curves [11,12].

Statistical analysis: All experiments were performed in triplicate (n = 3), with data presented as mean ± standard deviation (SD). Statistical analysis was conducted using one-way ANOVA followed by Tukey's post hoc test, with $p < 0.05$ considered statistically significant.

RESULTS AND DISCUSSION

Phytochemical screening: Qualitative phytochemical screening of the aqueous leaf extract of *L. aspera* revealed saponins, tannins, carbohydrates, flavonoids, glycolysis-related compounds, alkaloids, phenols and steroids, whereas terpenoids, amino acids, resins and phlobatannins were not detected. The observed profile differs in some respects from earlier reports, which can be attributed to differences in plant part, extraction solvent, geographical origin and extraction conditions. Rahman & Islam [13] reported alkaloids, glycosides, terpenoids, flavonoids, steroids, tannins, saponins and phlobatannins in whole plant extracts of *L. aspera*. Latha *et al*. [14] identified alkaloids, flavonoids, steroids, cardiac glycosides, saponins and tannins in different extracts of the plant. The absence of terpenoids and resins in the present aqueous extract may be related to the preferential extraction of polar constituents by water, whereas lipophilic compounds are generally recovered more efficiently with less polar solvents [13,14].

The presence of phenolic and flavonoid constituents is relevant to the green synthesis of AgNPs, since hydroxyl containing phytochemicals can participate in the reduction of Ag^+ ions and subsequent surface stabilization of the nanoparticles [15]. Alkaloids, tannins, saponins and reducing metabolites may contribute to these processes through their interactions with Ag^+ ions and the nanoparticle surface. The phytochemical profile of the extract, therefore, provides a chemical basis for its role as a natural reducing and capping medium.

GC-MS analysis: GC-MS analysis provided further insight into the chemical composition of the extract (Fig. 1). Twenty-five compounds were tentatively identified from their mass spectral fragmentation patterns and comparison with the NIST library (Table-1). The identified metabolites comprised fatty acids, terpenoids, sterols, alcohols, organic acids and sugar derivatives. Major constituents included lupeol, stigmast-5-en-3β-ol (β-sitosterol), retinyl palmitate, γ-linolenic acid, hexadecanoic acid (palmitic acid), octadecanoic acid (stearic acid) and dodecanoic acid (lauric acid). Glycerol, 2,3-butanediol, lactic acid and isosorbide were among the lower molecular weight metabolites detected.

The occurrence of fatty acids and sterol derivatives is consistent with previous investigations of *L. aspera*. Parimaladevi

TABLE-1
GC-MS ANALYSIS DATA OF AQUEOUS LEAF EXTRACT OF *L. aspera*

S. No.	Retention time (min)	Identified compound	m.f.
1	3.072	3-Methyl-1-butanol/isovaleric acid	$C_5H_{12}O/C_5H_{10}O_2$
2	3.800	Glycerol (glycerine)	$C_3H_8O_3$
3	5.108	2,3-Butanediol	$C_4H_{10}O_2$
4	7.544	Lactic acid (2-hydroxypropanoic acid)	$C_3H_6O_3$
5	8.032	6-Oxabicyclohexan-3-one	$C_5H_6O_2$
6	13.098	Hydroxy substituted anhydro sugar derivative	$C_6H_8O_4$
7	14.608	Isosorbide	$C_6H_{10}O_4$
8	16.122	6-Dodecanone	$C_{12}H_{24}O$
9	21.124	Dodecanoic acid (lauric acid)	$C_{12}H_{24}O_2$
10	21.738	Hexadecane	$C_{16}H_{34}$
11	23.373	Heptadecane	$C_{17}H_{36}$
12	24.350	Tetradecanoic acid (myristic acid)	$C_{14}H_{28}O_2$
13	25.300	Nucleoside derivative	$C_{10}H_{11}N_2O_6BrF_2$
14	26.767	Methyl hexadecanoate (methyl palmitate)	$C_{17}H_{34}O_2$
15	27.026	9-Hexadecenoic acid (palmitoleic acid)	$C_{16}H_{32}O_2$
16	27.322	Hexadecanoic acid (palmitic acid)	$C_{16}H_{32}O_2$
17	29.448	γ-linolenic acid	$C_{18}H_{30}O_2$
18	30.000	Octadecanoic acid (stearic acid)	$C_{18}H_{36}O_2$
19	36.467	Retinyl palmitate (vitamin A palmitate)	$C_{36}H_{60}O_2$
20	36.945	D-Glucitol hexaacetate (sorbitol hexaacetate)	$C_{18}H_{26}O_{12}$
21	37.232	Stigmast-5-en-3β-ol (β-sitosterol)	$C_{29}H_{50}O$
22	38.933	2,6-Lutidine	C_7H_9N
23	39.058	Lupeol	$C_{30}H_{50}O$
24	39.575	2,7-Dimethyloctanoic acid	$C_{10}H_{20}O_2$
25	39.912	Pentacyclic triterpenoid derivative	$C_{30}H_{48}O$

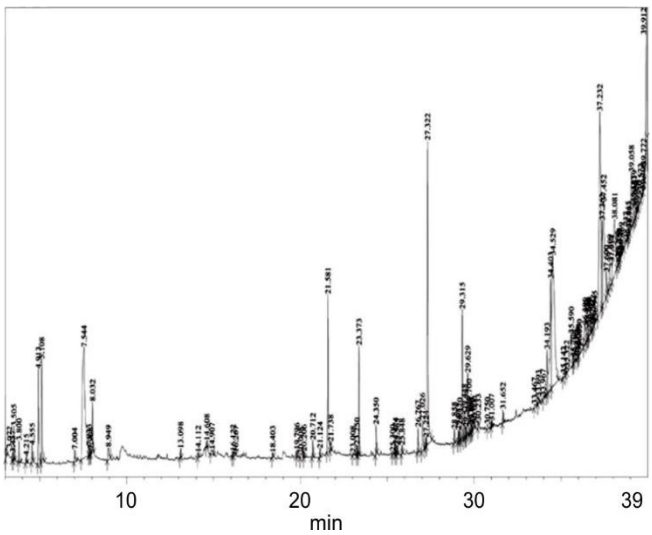

Fig. 1. GC-MS spectrum of aqueous leaf extract of *L. aspera*

et al. [16] reported fatty acids and sterol compounds in aqueous extracts of *L. aspera* and associated these constituents with antioxidant and cytotoxic properties. Begum & Sankarram [17] identified octadecanoic acid and hexadecanoic acid as major constituents in the hexane extract of *L. aspera*. The detection of palmitic acid, stearic acid, β-linolenic acid and lauric acid in the present extract is consistent with the fatty acid-rich profile reported for this species. β-Sitosterol and lupeol are of particular interest since β-sitosterol has been associated with antioxidant, anti-inflammatory and immunomodulatory activities [18], while lupeol has reported antimicrobial, anti-inflammatory, anticancer and neuroprotective properties [19]. These phytoconstituents may contribute to the biological properties of the extract and the phytochemical functionalization of the resulting AgNPs.

UV-Visible studies: The formation of AgNPs using *L. aspera* aqueous leaf extract was confirmed by UV-Visible spectroscopy (Fig. 2). A characteristic SPR band appeared at 415 nm, consistent with the optical response of nanoscale metallic silver. Smitha *et al*. [20] reported an SPR peak around 410 nm for *L. aspera*-mediated AgNPs, while Vijayaraj *et al*. [21] reported AgNPs formation through a characteristic colour change accompanied by visible absorption. AgNPs synthesized using *E. chapmaniana* and *L. reticulata* have likewise

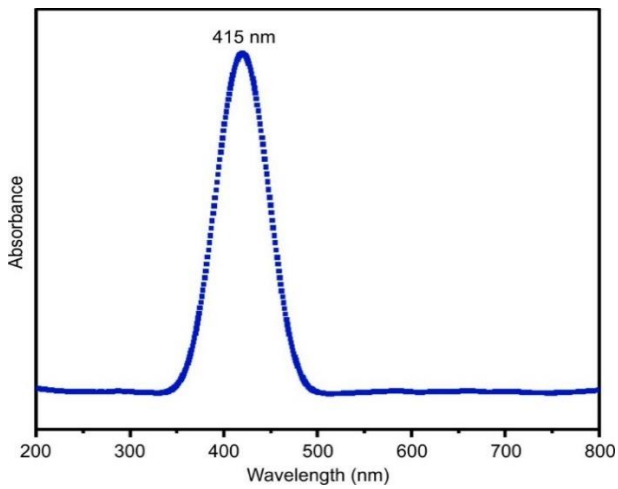

Fig. 2. UV-Vis spectrum of AgNPs synthesized from aqueous leaf extract of *L. aspera*

exhibited SPR responses within the visible region [22,23]. Vanlalveni *et al*. [24] reported that spherical AgNPs commonly display SPR absorption between 400 and 460 nm. The single prominent band at 415 nm supports AgNPs formation under the present synthesis conditions. The absence of distinct additional absorption bands suggests that no major optically active impurities were present in the analyzed sample.

XRD studies: XRD analysis established the crystalline nature and phase composition of the synthesized AgNPs (Fig. 3). Diffraction peaks at approximately 38.1º, 44.3º, 64.5º and 77.5º were indexed to the (111), (200), (220) and (311) planes, respectively, of face-centered cubic metallic Ag according to JCPDS file no. 04-0783 [25]. The intense (111) reflection at 38.1º represents the dominant crystallographic plane in the observed pattern.

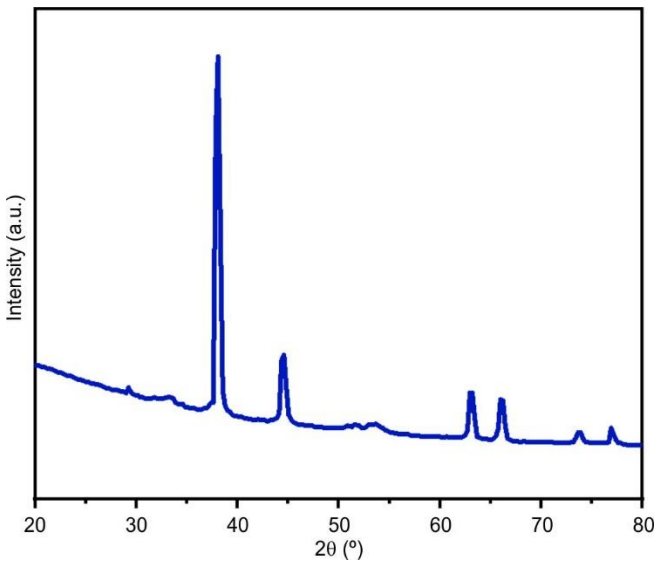

Fig. 3. XRD spectrum of AgNPs synthesized using aqueous leaf extract of *L. aspera*

The average crystallite size calculated from peak broadening using the Debye-Scherrer equation was 86.08 nm. Smitha *et al*. [20] reported a smaller crystallite size of ~36 nm for *L. aspera*-derived AgNPs. Differences in crystallite dimensions can arise from variations in extract concentration, silver precursor concentration, reaction temperature, reaction time and incubation conditions, which affect nucleation and crystal growth [24]. The well-defined Ag reflections and absence of additional major crystalline phases support the formation of crystalline metallic Ag.

FTIR studies: FTIR spectra of the *L. aspera* extract and synthesized AgNPs are shown in Fig. 4. The extract exhibited a broad band at 3508.96 cm^{-1} assigned to O–H stretching, while the band at 2945.2 cm^{-1} corresponded to aliphatic C–H stretching. Bands at 1623.48 and 1503.04 cm^{-1} were associated with carbonyl/aromatic C=C vibrations, while absorptions at 1153.74, 953.1 and 532.8 cm^{-1} occurred in the fingerprint region and were associated with C–O and other molecular vibrations.

The AgNPs spectrum retained several characteristic functional-group bands, with absorptions at 3419.98 cm^{-1} (O–H), 2922.01 cm^{-1} (C–H), 1616.19 cm^{-1} (C=C/carbonyl associated vibrations), 1453.78 cm^{-1}, 1387.89 cm^{-1} and 1052.44 cm^{-1}. The shifts and intensity changes observed after nanoparticle formation point to interactions between phytochemical functional groups and the AgNP surface. Liaqat *et al*. [26] reported comparable spectral changes in *Terminalia arjuna*-mediated AgNPs and associated them with polyphenols, flavonoids, proteins and alkaloids. Raut *et al*. [27] likewise reported the involvement of hydroxyl- and carbonyl-containing compounds in Ag^{+} reduction and nanoparticle stabilization. The present FTIR findings support the participation of phenolic, flavonoid and other oxygen containing phytochemicals in AgNPs formation and surface stabilization.

Morphological studies: SEM analysis revealed irregular to near-spherical AgNPs with some degree of aggregation (Fig. 5a). The observed morphology may be related to interactions among surface-associated phytochemicals and the nanoparticles [24]. Particle-size analysis from the SEM micrograph gave an average size of 65.82 nm (Fig. 5b), confirming the nanoscale dimensions of the material.

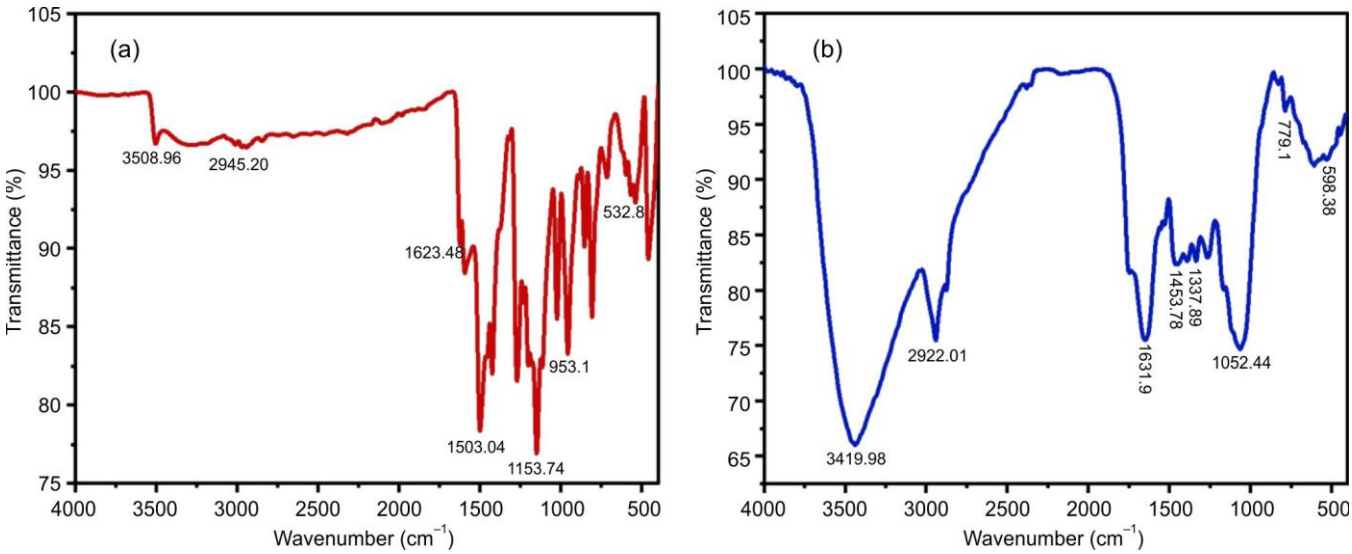

Fig. 4. FTIR spectrum of (a) leaf extract of *L. aspera* and (b) AgNPs synthesized using aqueous leaf extract of *L. aspera*

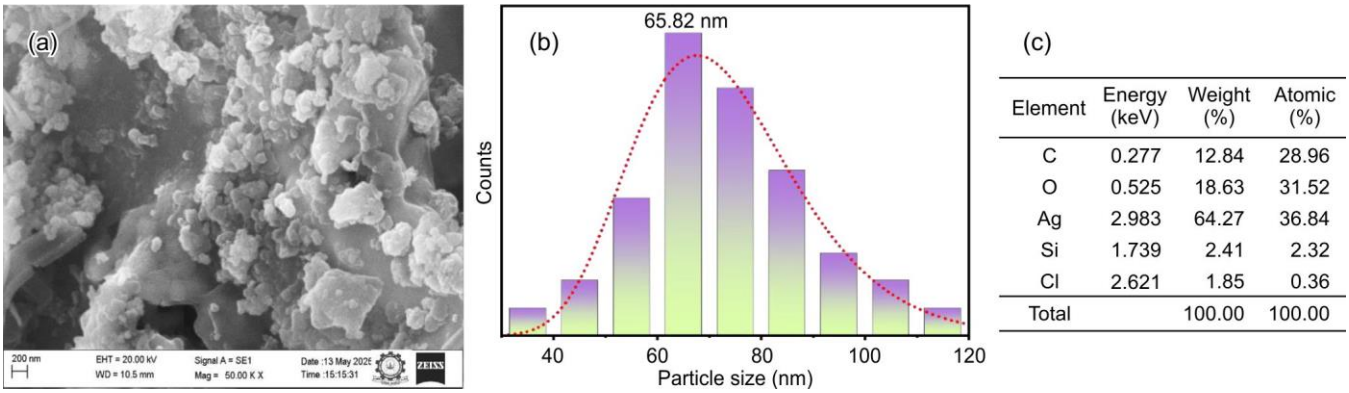

(c)

Element	Energy (keV)	Weight (%)	Atomic (%)
C	0.277	12.84	28.96
O	0.525	18.63	31.52
Ag	2.983	64.27	36.84
Si	1.739	2.41	2.32
Cl	2.621	1.85	0.36
Total		100.00	100.00

Fig. 5. (a) SEM image, (b) particle size distribution and (c) EDX elemental analysis of green synthesized AgNPs using aqueous leaf extract of *L. aspera*

EDX analysis confirmed Ag as the predominant elemental component, with a characteristic Ag signal at ~2.983 keV (Fig. 5c). The elemental composition comprised 64.27 wt.% Ag (36.84 at.%), carbon (12.84 wt.%) and oxygen (18.63 wt.%), together with minor silicon and chlorine signals. Carbon and oxygen may arise from phytochemical residues associated with the nanoparticle surface and are consistent with the presence of an organic capping layer [28]. The SEM and EDX findings support the formation of nanoscale, phytochemically capped Ag particles, with Ag as the principal detected element.

DLS and zeta potential: DLS analysis gave an average hydrodynamic diameter of 118.74 nm (Fig. 6), which was higher than the SEM-derived particle size of 65.82 nm. This difference is expected since DLS measures the hydrodynamic dimension of particles dispersed in liquid, encompassing the metallic core, surface-bound phytochemicals and associated solvent layer [28]. The result is consistent with the presence of a phytochemical corona surrounding the AgNPs.

The zeta potential was -26.78 mV, confirming the presence of a negatively charged nanoparticle surface. This negative surface charge may arise from ionizable oxygen containing functional groups associated with phenolic, flavonoid and other plant-derived constituents. Electrostatic repulsion between similarly charged particles can limit aggregation and support colloidal stability. Khandel *et al.* [29] reported a zeta potential of -19.4 mV for *Alpinia calcarata*-derived AgNPs, while Ashraf *et al.* reported -22.3 mV for *Melia azedarach*-mediated AgNPs [30]. The present value is within a comparable range and supports the contribution of plant-derived molecules to AgNP surface stabilization.

Antibacterial activity: The antibacterial activity of *L. aspera*-mediated AgNPs was evaluated against *S. aureus* and *P. aeruginosa* using the agar well diffusion assay (Table-2). A concentration-dependent increase in inhibition was observed for both organisms. *S. aureus* exhibited inhibition zones of 16, 18, 20 and 22 mm at 10, 15, 20 and 25 µL, respectively. For *P. aeruginosa*, no inhibition was observed at 10 µL, whereas inhibition zones of 12, 16 and 19 mm were recorded at 15, 20 and 25 µL, respectively. The positive control produced inhibition zones of 25 and 24 mm against *S. aureus* and *P. aeruginosa*, respectively.

S. aureus exhibited higher susceptibility than *P. aeruginosa* at the tested doses. Differences in cell-envelope architecture may account for this response. The peptidoglycan-rich envelope of Gram-positive bacteria provides a different interaction environment from the lipopolysaccharide-containing outer

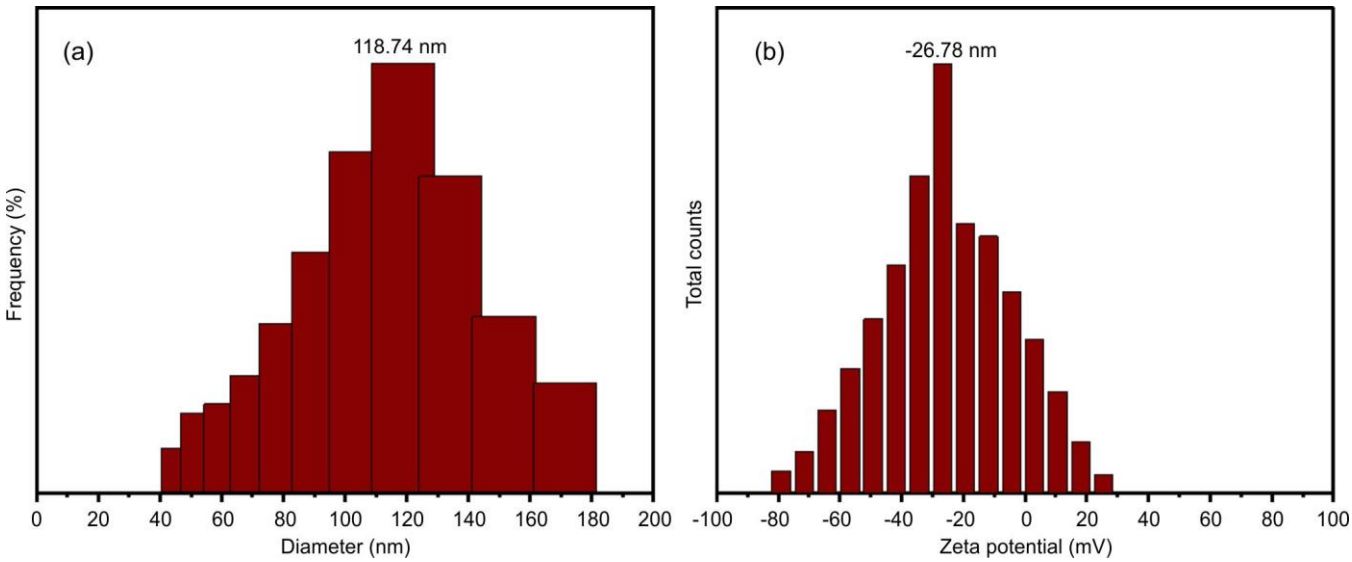

Fig. 6. Hydrodynamic diameter and zeta potential analysis of synthesized AgNPs using aqueous leaf extract of *L. aspera*

TABLE-2
ANTIBACTERIAL ACTIVITY DATA OF GREEN SYNTHESIZED AgNPs USING AQUEOUS LEAF EXTRACT OF *L. aspera* AGAINST *S. aureus* AND *P. aeruginosa*

Pathogens	Zone of inhibition (mm)				Positive control
	10 µL	15 µL	20 µL	25 µL	
S. aureus	16	18	20	22	25
P. aeruginosa	–	12	16	19	24

membrane of Gram-negative bacteria, which can restrict nanoparticle interaction and penetration [24,28,31]. The antibacterial activity of green synthesized AgNPs has been associated with membrane disruption, ROS generation, protein dysfunction and DNA damage [32]. Qayyum *et al.* [32] linked green-synthesized AgNPs activity to ROS-mediated oxidative stress and membrane damage, while Roy *et al.* [33] reported that phytochemical-coated AgNPs can exert antimicrobial effects through the combined activity of silver ions and plant-derived molecules. The antibacterial response observed in the present study may involve both silver-mediated effects and the contribution of phytochemicals associated with the nanoparticle surface.

MIC and MBC measurements further supported the antibacterial activity (Table-3). The MIC and MBC values were 100 and 125 µg/mL respectively, giving an MBC/MIC ratio of 1.25. This ratio is consistent with a bactericidal response and supports the antibacterial potential of the synthesized AgNPs against the tested organisms.

TABLE-3
DETERMINATION OF MIC AND MBC VALUES OF *L. aspera* LEAF EXTRACT-MEDIATED AgNPs

Bacterial strain	MIC (µg/mL)	MBC (µg/mL)	MBC/MIC ratio	Antibacterial nature
S. aureus	20	25	1.25	Bactericidal
P. aeruginosa	20	25	1.25	Bactericidal

Anticancer activity: The cytotoxic potential of the *L. aspera* aqueous extract and synthesized AgNPs was evaluated against HEp-2 human laryngeal carcinoma cells using the MTT assay. Cells were treated with 25, 50, 100, 200 and 400 µg/mL of the extract or AgNPs for 24 h. The MTT assay measures cellular metabolic activity through the reduction of MTT to purple formazan by viable cells. Both treatments caused a concentration-dependent reduction in cell viability compared with untreated cells.

L. aspera extract reduced HEp-2 cell viability from 92.47 ± 4.78% at 25 µg/mL to 46.89 ± 5.71% at 400 µg/mL. AgNPs treatment reduced viability from 84.63 ± 1.56% to 33.63 ± 3.48% over the same concentration range (Fig. 7). The IC_{50} values were 355.36 µg/mL for the *L. aspera* extract and 236.63 µg/mL for the AgNPs. The lower IC_{50} of the AgNPs indicates higher cytotoxic potency against HEp-2 cells under the experimental conditions. Satyavani *et al.* [34] reported concentration-dependent cytotoxicity of AgNPs against HEp-2 cells and associated the response with oxidative stress and apoptosis. Husen & Siddiqi [35] likewise reported concentration- and exposure-dependent cytotoxicity of biosynthesized AgNPs.

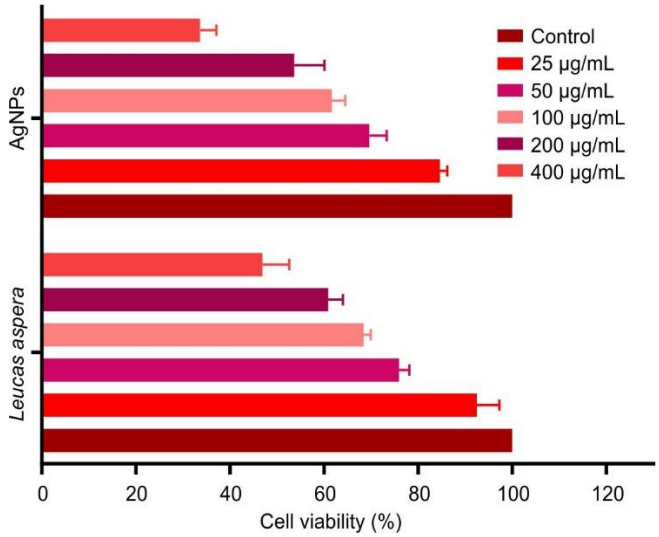

Fig. 7. Cytotoxic effect of *L. aspera* and AgNPs on HEp-2 human laryngeal cancer cells assessed by MTT assay [Data are expressed as mean ± SD of three independent experiments. Statistical significance was considered at $p < 0.05$ compared with the untreated control group]

ROS generation, mitochondrial dysfunction, DNA damage and apoptotic signalling have been implicated in the cytotoxic effects of AgNPs. Satyavani *et al.* [34] reported ROS generation, mitochondrial damage and DNA fragmentation in HEp-2 cells following AgNP exposure. Rosarin *et al.* [36] and Mukherjee *et al.* [37] associated plant-derived AgNPs cytotoxicity with oxidative stress and apoptosis. Al-Khedhairy & Wahab [38] reported increased levels of pro-apoptotic markers such as p53, Bax and caspase-3, together with decreased Bcl-2 expression following AgNPs treatment. ROS-dependent apoptotic responses have likewise been reported by Zhu *et al.* [39] and Buttacavoli *et al.* [40]. The higher cytotoxicity observed for the *L. aspera*-mediated AgNPs than for the crude extract may arise from the combined effects of nanosilver and surface-associated phytochemicals, although specific mechanistic assays would be required to establish the contribution of individual apoptotic pathways.

Conclusion

The present study established an eco-friendly approach for synthesizing AgNPs using aqueous leaf extract of *Leucas aspera*. Phytochemicals present in the extract participated in Ag^+ reduction and nanoparticle stabilization, yielding crystalline and biofunctionalized AgNPs. UV-Visible, XRD, FTIR, SEM, EDX, DLS and zeta potential analyses confirmed their physicochemical characteristics and colloidal stability. The synthesized AgNPs exhibited concentration-dependent antibacterial activity against both Gram-positive and Gram-negative bacteria, with MIC and MBC results supporting a bactericidal

effect. AgNPs further exhibited higher cytotoxic activity against HEp-2 laryngeal carcinoma cells than the *L. aspera* extract, as evidenced by the lower IC_{50} value. These findings support the potential of *L. aspera*-mediated AgNPs as biofunctional nanomaterials for antimicrobial and cancer-related applications.

CONFLICT OF INTEREST

The authors declare that there is no conflict of interests regarding the publication of this article.

DECLARATION OF AI-ASSISTED TECHNOLOGIES

During the preparation of this manuscript, the authors used an AI-assisted tool(s) to improve the language and no data, results or scientific conclusions were generated by AI. All analyses, interpretations and conclusions are the authors' own. The authors reviewed and edited the content and take full responsibility for the published work.

REFERENCES

1. A. Sati, T.N. Ranade, S.N. Mali, H.K. Ahmad Yasin and A. Pratap, *ACS Omega*, **10**, 7549 (2025); https://doi.org/10.1021/acsomega.4c11045
2. M. Bhange and D. Telange, *Discov. Oncol.*, **16**, 77 (2025); https://doi.org/10.1007/s12672-025-01821-y
3. F. Zanbili and A. Poursattar Marjani, *Micro Nano Systems Lett.*, **13**, 3 (2025); https://doi.org/10.1186/s40486-025-00223-7
4. M. Harun-Ur-Rashid, T. Foyez, S.B. Krishna, S. Poda and A.B. Imran, *RSC Adv.*, **15**, 8480 (2025); https://doi.org/10.1039/D4RA08220F
5. E. Dube and G.E. Okuthe, *Microbiol. Res.*, **16**, 110 (2025); https://doi.org/10.3390/microbiolres16060110
6. K. Shagirtha, M. Divya, M.K. Srinivasan, S. Alamelu, K.B. Venkatesan, M. Sivaprakasam, C. Panneerselvam, M.A. Alshehri, L.A. Alshuraym and S. Sayed, *J. Pak. Bot.*, **57**, 1033 (2025); https://doi.org/10.30848/PJB2025-3(26)
7. J.B. Harborne, Phytochemical Methods: A Guide to Modern Techniques of Plant Analysis, London, U.K.: Chapman and Hall, edn 3, pp. 302 (1998).
8. W.C. Evans, Trease and Evans' Pharmacognosy, Edinburgh, U.K.: Saunders/Elsevier, edn 16 (2009).
9. A. Wirwis and Z. Sadowski, *ACS Omega*, **8**, 30532 (2023); https://doi.org/10.1021/acsomega.3c03775
10. M.Y. Begum, M. Sharma, M.V. Arularasu, P. Vinitha, V. Vetrivelan, G. Kandasamy, A. Manikandan, A.G. Ayanie, L. Gnanasekaran, A. Mehta and R. Gupta, *RSC Adv.*, **15**, 50582 (2025); https://doi.org/10.1039/d5ra08168h
11. M.K. Srinivasan and N. Namasivayam, *J. Biomater. Sci. Polym. Ed.*, **36**, 796 (2025); https://doi.org/10.1080/09205063.2024.2429325
12. A. Vasanthakumar, S. Priyadharshini, K.B. Venkatesan, M. Ayyanar, A. Thirumurugan and N. Chidhambaram, *Next Mater.*, **12**, 102365 (2026); https://doi.org/10.1016/j.nxmate.2026.102365
13. M.A. Rahman and M.S. Islam, *Asian Pac. J. Trop. Biomed.*, **3**, 273 (2013); https://doi.org/10.1016/S2221-1691(13)60062-3
14. B.M. Latha, Y. Rumaisa, C. Soumya, S. Shahul and N. Sadhiya, *J. Chem. Pharm. Res.*, **5**, 222 (2013).
15. S. Medici, M. Peana, V.M. Nurchi and M.A. Zoroddu, *J. Med. Chem.*, **62**, 5923 (2019); https://doi.org/10.1021/acs.jmedchem.8b01439
16. S.T. Parimaladevi, D.R. Chellappan, V.T. Sudha and P. Brindha, *Asian J. Chem.*, **26**, 3675 (2014); https://doi.org/10.14233/ajchem.2014.17052
17. F.M. Begum and M. Sankarram, *Biotechnologia*, **105**, 55 (2024); https://doi.org/10.5114/bta.2024.135642
18. S.L. Khan and F.A. Siddiqui, *Arch. Pharmacol. Ther.*, **2**, (2020); https://doi.org/10.33696/Pharmacol.2.014
19. A. Parvez, M.A. Rahman, M.M. Rahman, A.I. Shimki, S. Ahmmed, F.A. Supti, M.H. Hasan, M.S.A. Bristi, S.A. Ansari and M.T. Islam, *Chem. Biodivers.*, **22**, e202402286 (2025); https://doi.org/10.1002/cbdv.202402286
20. V. Smitha, M. Priyadharshana, M. Girija, M.A. Badhsheeba and V. Vadivel, *J. Life Sci.*, **7**, 85 (2022); https://doi.org/10.36348/sjls.2022.v07i03.003
21. D. Vijayaraj, J. Anarkali, K. Rajathi and S. Sridhar, *Nano Biomed. Eng.*, **4**, 95 (2012); https://doi.org/10.5101/nbe.v4i2.p95-98
22. G.M. Sulaiman, W.H. Mohammed, T.R. Marzoog, A.A. Al-Amiery, H. Kadhum and A.B. Mohamad, *Asian Pac. J. Trop. Biomed.*, **3**, 58 (2013); https://doi.org/10.1016/S2221-1691(13)60024-6
23. M.K. Swamy, K.M. Sudipta, K. Jayanta and S. Balasubramanya, *Appl. Nanosci.*, **5**, 73 (2014); https://doi.org/10.1007/s13204-014-0293-6
24. C. Vanlalveni, S. Lallianrawna, A. Biswas, M. Selvaraj, B. Changmai and S.L. Rokhum, *RSC Adv.*, **11**, 2804 (2021); https://doi.org/10.1039/D0RA09941D
25. M.V. Arularasu, M.S. Ramkumar, R. Tarunprasad and P. Vinitha, *Sens. Biosensing Res.*, **49**, 100837 (2025); https://doi.org/10.1016/j.sbsr.2025.100837
26. N. Liaqat, N. Jahan, Khalil-ur-Rahman, T. Anwar and H. Qureshi, *Front. Chem.*, **10**, 952006 (2022); https://doi.org/10.3389/fchem.2022.952006
27. R.W. Raut, N.S. Kolekar, J. Lakkakula, V.D. Mendhulkar and S.B. Kashid, *Nano-Micro Lett.*, **2**, 106 (2010); https://doi.org/10.1007/BF03353627
28. S. Ghasemi, S. Dabirian, F. Kariminejad, D.E. Koohi, M. Nemattalab, S. Majidimoghadam, E. Zamani and F. Yousefbeyk, *Sci. Rep.*, **14**, 4130 (2024); https://doi.org/10.1038/s41598-024-54702-9
29. P. Khandel, S.K. Shahi, D.K. Soni, R.K. Yadaw and L. Kanwar, *Nano Converg.*, **5**, 37 (2018); https://doi.org/10.1186/s40580-018-0167-9
30. H. Ashraf, T. Anjum, S. Riaz and S. Naseem, *Front. Microbiol.*, **11**, 238 (2020); https://doi.org/10.3389/fmicb.2020.00238
31. C. Panneerselvam, A. Alasmari, R.F. Affan, Z.M. Mohammedsaleh, K.B. Venkatesan and K. Kaliyamoorthi, *Discov. Nano*, **21**, 278 (2026); https://doi.org/10.1186/s11671-026-04737-w
32. S. Qayyum, M. Oves and A.U. Khan, *PLoS One*, **12**, e0181363 (2017); https://doi.org/10.1371/journal.pone.0181363
33. A. Roy, O. Bulut, S. Some, A.K. Mandal and M.D. Yilmaz, *RSC Adv.*, **9**, 2673 (2019); https://doi.org/10.1039/C8RA08982E
34. K. Satyavani, G. Selvaraj, T. Ramanathan and T. Balasubramanian, *J. Nanobiotechnology*, **9**, 43 (2011); https://doi.org/10.1186/1477-3155-9-43
35. A. Husen and K.S. Siddiqi, *Nanoscale Res. Lett.*, **9**, 229 (2014); https://doi.org/10.1186/1556-276X-9-229
36. F.S. Rosarin, V. Arulmozhi, S. Nagarajan and S. Mirunalini, *Asian Pac. J. Trop. Med.*, **6**, 1 (2013); https://doi.org/10.1016/S1995-7645(12)60193-X
37. S. Mukherjee, D. Chowdhury, R. Kotcherlakota, B. Vinothkumar, S. Patra, M.P. Bhadra, B. Sreedhar and C.R. Patra, *Theranostics*, **4**, 316 (2014); https://doi.org/10.7150/thno.7819
38. A.A. Al-Khedhairy and R. Wahab, *Metals*, **12**, 148 (2022); https://doi.org/10.3390/met12010148
39. B. Zhu, Y. Li, Z. Lin, M. Zhao, T. Xu, C. Wang and N. Deng, *Nanoscale Res. Lett.*, **11**, 198 (2016); https://doi.org/10.1186/s11671-016-1419-4
40. M. Buttacavoli, N.N. Albanese, G. Di Cara, R. Alduina, C. Faleri, M. Gallo, G. Pizzolanti, G. Gallo, S. Feo, F. Baldi and P. Cancemi, *Oncotarget*, **9**, 9685 (2018); https://doi.org/10.18632/oncotarget.23859